Journal of Bone and Mineral Metabolism (2023) 41:752–759
https://doi.org/10.1007/s00774-023-01460-9

ORIGINAL ARTICLE

Deterioration of apatite orientation in the cholecystokinin B receptor gene (Cckbr)-deficient mouse femurs

Yuki Mihara[1] · Takuya Ishimoto[2] · Ryosuke Ozasa[2] · Takao Omura[1] · Yu Yamato[1] · Tomohiro Yamada[1] · Ayako Okamoto[1] · Yukihiro Matsuyama[1] · Takayoshi Nakano[2]

Received: 20 April 2023 / Accepted: 20 July 2023 / Published online: 7 September 2023

Abstract

Introduction The discrepancy between bone mineral density (BMD), the gold standard for bone assessment, and bone strength is a constraint in diagnosing bone function and determining treatment strategies for several bone diseases. Gastric hypochlorhydria induced by clinically used proton pump inhibitor (PPI) therapy indicates a discordance between changes in BMD and bone strength. Here, we used Cckbr-deficient mice with gastric hypochlorhydria to examine the effect of gastric hypochlorhydria on bone mass, BMD, and preferential orientation of the apatite crystallites, which is a strong indicator of bone strength.

Materials and methods Cckbr-deficient mice were created, and their femurs were analyzed for BMD and preferential orientation of the apatite *c*-axis along the femoral long axis.

Results Cckbr-deficient mouse femurs displayed a slight osteoporotic bone loss at 18 weeks of age; however, BMD was comparable to that of wild-type mice. In contrast, apatite orientation in the femur mid-shaft significantly decreased from 9 to 18 weeks. To the best of our knowledge, this is the first report demonstrating the deterioration of apatite orientation in the bones of Cckbr-deficient mice.

Conclusion Lesions in Cckbr-deficient mice occurred earlier in apatite orientation than in bone mass. Hence, bone apatite orientation may be a promising method for detecting hypochlorhydria-induced osteoporosis caused by PPI treatment and warrants urgent clinical applications.

Keywords Cckbr-deficient mice · Bone quality · Apatite orientation · Hypochlorhydria · Bone evaluation

Introduction

The dissociation between bone mineral density (BMD) and bone strength has been reported in both human and animal bones subjected to bone disorders, including fracture healing [1, 2], osteoporosis [3, 4], osteopetrosis [5], rheumatoid bone [6, 7], and metastasis [8]. These studies demonstrated that bone quantity measurement alone is not sufficient to determine bone strength. To clarify the dissociation between bone mineral quantity and bone strength, extracellular matrix (ECM) quality should be considered [9]. Previously, we reported that the preferential orientation of the ECM, which is mainly composed of organic collagen fibers and inorganic apatite crystallites, is an important determinant of bone material integrity [10, 11]. Collagen and apatite exhibit anisotropic mechanical properties; the collagen fiber direction and apatite crystallographic *c*-axis display the highest strength. In the normal mineralization of bone, the crystallographic *c*-axis of apatite is aligned approximately parallel to the collagen fiber direction. This results in an oriented nanocomposite in which the strong directions of the two materials are aligned [12, 13]. Highly oriented apatite *c*-axes and collagen fibers mainly contribute to bone stiffening [11] and toughening [14], respectively. Therefore, evaluation of

✉ Yukihiro Matsuyama
spine-yu@hama-med.ac.jp

✉ Takayoshi Nakano
nakano@mat.eng.osaka-u.ac.jp

[1] Department of Orthopedic Surgery, Hamamatsu University School of Medicine, 1-20-1, Handayama, Higashi-Ku, Hamamatsu, Shizuoka 431-3192, Japan

[2] Division of Materials and Manufacturing Science, Graduate School of Engineering, Osaka University, 2-1, Yamada-Oka, Suita, Osaka 565-0871, Japan

the preferential orientation of the bone ECM is important when discussing the fragility of pathological bones.

More than 20% of osteoporotic fracture patients were treated with proton pump inhibitors (PPI) to reduce the risk of the gastrointestinal side effects of bisphosphonates [15], which are the commonest medicines for osteoporosis. However, the negative effects of hypochlorhydria on bone properties were investigated using Cckbr-deficient mice [16]. Cckbr-deficient mice exhibit gastric hypochlorhydria and calcium malabsorption. Calcium deficiency leads to secondary hyperparathyroidism and excessive bone resorption, resulting in an osteoporotic phenotype. Cckbr-deficient mice demonstrate osteoporotic changes, characterized by an increase in osteoclasts on the bone surface, loss of bone volume and cortical bone thickness, elevated concentrations of bone-specific collagen degradation products, and decreased power endurance [16]. Cckbr-deficient mice showed secondary hyperparathyroidism at as early as 2 weeks of age, a marked decrease in BV/TV of the vertebral body at 12 weeks, and severe cortical porosity even in the cortical bone of tibia and femur at 52 weeks of age [16].

Osteoporosis has been reported to cause not only a decrease in BMD but also changes in ECM orientation that also significantly affects bone strength [17]. We hypothesized that ECM orientation is affected by Cckbr-deficiency-induced osteoporotic conditions. Therefore, the purpose of this novel study was to evaluate the preferential orientation of ECM as a bone quality parameter in Cckbr-deficient and wild-type mice. Since cases of ECM orientation being more acutely altered than BMD was in response to physiological changes have been reported [18], 9- and 18-week-old mice, before and after 12 weeks of age, when BV/TV was reduced, were used in this study. If a steeper change in ECM orientation than that in BMD is observed, it would be clinically significant from the perspective of the early detection of bone abnormalities. Additionally, gastric hypochlorhydria is caused by long-term proton pump inhibitor (PPI) therapy and is associated with an increased risk of osteoporosis [19]. Therefore, the analysis of these mice has important clinical implications.

Materials and methods

Animals

Jl embryonic stem (ES) cells were electroporated with a linearized targeting vector and selected with geneticin (G418) on embryonal fibroblast feeder cells. In total, 1033 G418-resistant clones were screened by Southern blot analysis using 5' external and 3' internal probes. Six clones showed evidence of homologous recombination of the disrupted Cckbr gene. Four ES clones were microinjected into the blastocysts of C57BL/6 J female mice. Two independent ES clones generated germline chimeras. Chimeras were bred with C57BL/6 J and 129sv mice to generate heterozygous mutant Fl mice [20]. We purchased these mice from the RIKEN BioResource Center. All the mice were housed in a colony room controlled for temperature and humidity with a 12:12-h light/dark cycle (lights on at 07:00 h) with food, 5001-Laboratory Rodent Diet (Land O'Lakes, MN, US), and water available ad libitum. Twenty mice (10 Cckbr-deficient and 10 wild–type) were used for the analyses. At 9 and 18 weeks of age ($N=5$), the animals were sacrificed using an overdose of sodium pentobarbital, and the right femur was harvested and immersed in a 75% ethanol solution to prevent denaturation of the organic constituents. The fourth lumbar vertebra was similarly sampled for the comparison of BMD changes with the femur.

All experiments were conducted according to protocols approved by the Animal Care and Use Committee of Hamamatsu University School of Medicine (approval number: 2019002).

Radiography

Soft X-ray photographs (XIE; Chubu Medical, Mie, Japan) were acquired after the femur was removed using 30 kV and 30 µA radiation.

Evaluation of volumetric BMD and cross-sectional area

Volumetric BMD and cross-sectional area were measured using a peripheral quantitative computed tomography (pQCT) (XCT Research SA + system; Stratec Medizintechnik GmbH, Birkenfeld, Germany) with a resolution of $70\times70\times260$ µm. This analysis was performed at regular intervals of 1/10th the bone length along the bone axis. The bone tissue was arbitrated to be above the threshold value of 690 mg/cm^3. In addition, the volumetric BMD of the transverse section at the height center of the fourth lumbar vertebra was measured under the same conditions. The threshold for bone tissue was set at 395 mg/cm^3, which is defined as the threshold for cancellous bone.

Analysis of apatite *c*-axis orientation (bone quality)

Because the apatite *c*-axis is oriented almost parallel to the collagen fiber direction, the apatite *c*-axis orientation mirrors the collagen fiber orientation [12, 13]. The degree of apatite *c*-axis orientation was analyzed using a microbeam X-ray diffractometer (µXRD) (R-Axis BQ; Rigaku, Tokyo, Japan) equipped with a transmission-type optical system and an imaging plate (storage phosphors) (Fuji Film, Tokyo, Japan) placed behind the specimen. Mo-Kα

radiation with a wavelength of 0.07107 nm was generated at a tube voltage of 50 kV and a tube current of 90 mA. The distance between the detector and the X-ray focus of the specimen was 127.4 mm and the pixel size of the imaging plate was 100 µm × 100 µm. Subsequently, the incident beam was radiated vertically to the long axis of the bone to detect diffraction along the bone axis. It was focused on a beam spot of 300 µm in diameter by a double-pinhole metal collimator and radiated in the anteroposterior axis from the anterior surface at the center of the bone width (Fig. 1a). The diffraction data were collected for 300 s. The analysis was performed at positions where the µXRD analysis was implemented. From the obtained diffraction intensity pattern (Debye ring) (Fig. 1b), two representative diffraction peaks of apatite (002) and (310) were used for apatite *c*-axis orientation analysis [21]. In long bones, the apatite *c*-axis is preferentially oriented along the longitudinal axis of the bone aligned with the collagen matrix [13]. Therefore, in this study, diffraction information along the long axis of the femur was analyzed. The upper and lower parts of the Debye ring correspond to the long axis of the femur (Fig. 1b). The diffraction intensities were azimuthally integrated into the range of 100 pixels to obtain an X-ray diffraction profile.

The degree of the preferential orientation of the apatite *c*-axis was determined as the relative intensity ratio of the (002) diffraction peak to the (310) peak in the X-ray profile. This has been reported as a suitable index for evaluating apatite orientation [10, 11]. Subsequently, the intensity ratios calculated for the upper and lower parts of the Debye ring were averaged. Randomly oriented hydroxyapatite (NIST #2910: calcium hydroxyapatite) powder had an intensity ratio of 0.8; therefore, the detected values > 0.8 indicated the presence of anisotropic apatite *c*-axis orientation in the analyzed direction.

Statistical analyses

Quantitative results are expressed as mean ± the standard deviation (SD). A two-tailed *t* test was used to compare data between Cckbr-deficient and wild-type mice. $P < 0.05$ was considered significant. SPSS version 25 software (SPSS Japan Inc., Tokyo, Japan) for Microsoft Windows was used for all statistical analyses.

Results

Shape of the femur

Figure 2 reveals the soft X-ray photographs of Cckbr-deficient and wild-type mice at 9 and 18 weeks of age. At 9 weeks, there were no obvious differences in the shape of the femoral bone between Cckbr-deficient and wild-type mice. In contrast, at 18 weeks of age, the femoral cortex appeared thin in Cckbr-deficient mice (Fig. 2). Cckbr-deficient mice had a significantly thinner cross-sectional femoral bone area at 18 weeks of age, whereas no significant differences were detected at 9 weeks of age (Fig. 3).

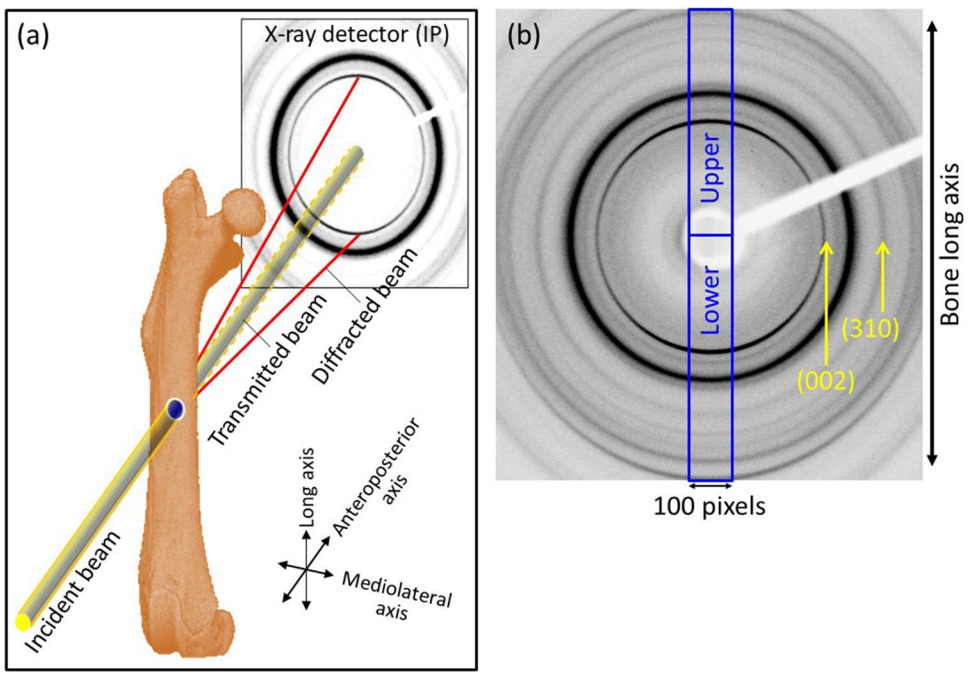

Fig. 1 µXRD analysis is performed in this study. **a** Schematic drawing of an optical system with the bone specimen and **b** a typical obtained µXRD pattern (Debye ring)

BMD

Cortical BMD minimally differed between Cckbr-deficient and wild-type female mouse femurs at 9 and 18 weeks of age, as shown in Fig. 4. On the other hand, vertebral BMD was significantly lower in Cckbr-deficient mice at 18 weeks of age (Fig. 5).

Apatite *c*-axis orientation along the bone long axis

Figure 6a depicts the degree of the apatite *c*-axis orientation, analyzed as the intensity ratio of (002)/(310) along the long bone axis. In the femurs of wild-type mice, the degree of apatite orientation peaked at the femoral mid-shaft and decreased toward the metaphysis. In contrast, Cckbr-deficient mouse femurs demonstrated a significantly lower degree of apatite *c*-axis orientation than that demonstrated by wild-type mouse femurs around the mid-shaft.

Discussion

This study measured and compared the density and preferential orientation of apatite at the bone tissue level in the femurs of Cckbr-deficient and wild-type mice. These measurements were performed on the cortical bone at the

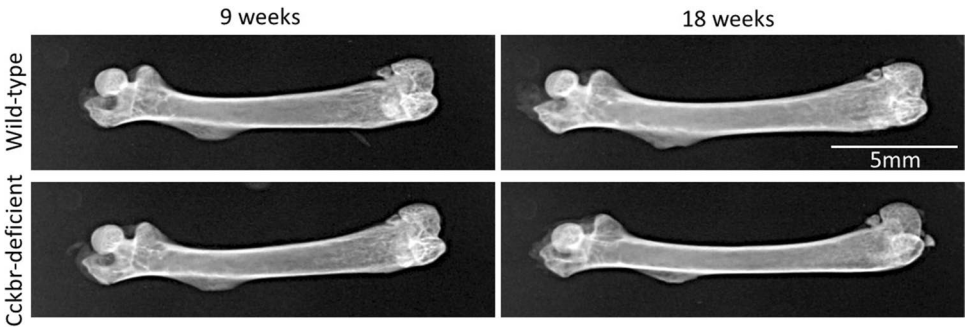

Fig. 2 Soft X-ray photographs of Cckbr-deficient and wild-type mouse femurs at 9 and 18 weeks of age

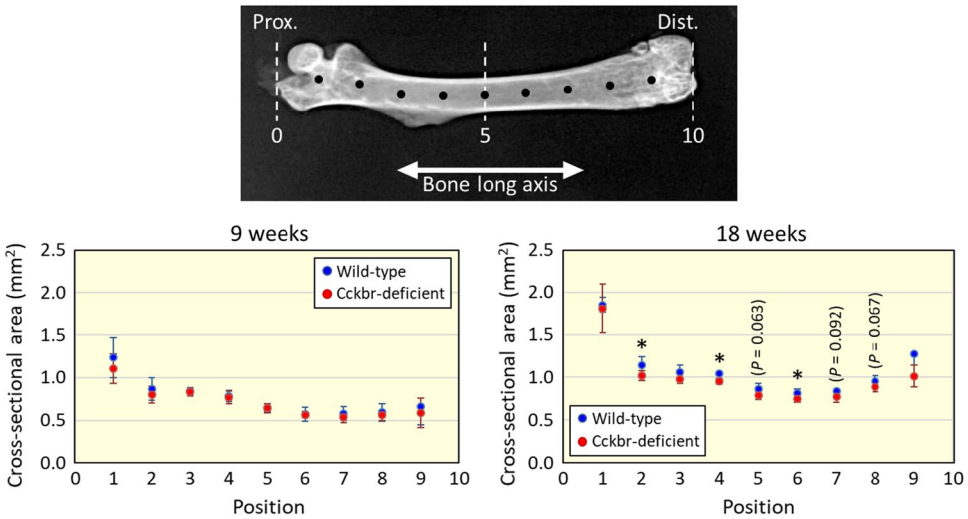

Fig. 3 Distribution of cross-sectional bone area of the femur along the bone long axis for Cckbr-deficient and wild-type mice. Analyzed points are indicated in soft X-ray photographs. *$P < 0.05$

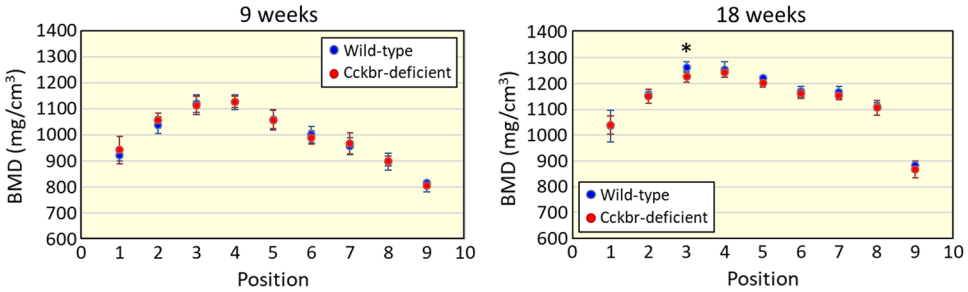

Fig. 4 Distribution of BMD of the femur along the bone long axis. *$P < 0.05$

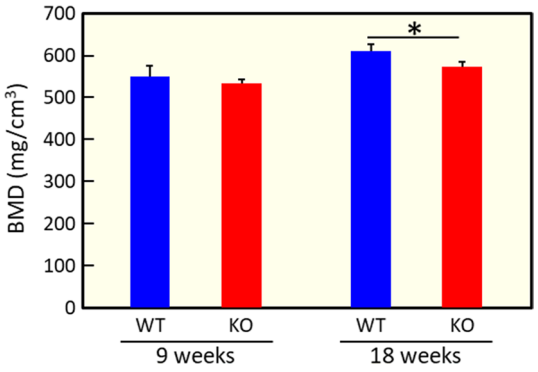

Fig. 5 BMD of the fourth lumbar vertebra in the central transverse section. $*P < 0.05$

mid-shaft of the femur. Our findings indicated a deterioration in apatite orientation in the femurs of Cckbr-deficient mice, without significant differences in volumetric BMD.

The volumetric BMD of the femoral diaphysis, which is composed almost entirely of cortical bone, is extremely sluggish in its response to metabolic disease compared to that associated with the spinal BMD [22]. In fact, vertebral BMD showed a decreasing trend at 9 weeks and was significantly lower at 18 weeks of age. Since rodent cortical bone lacks osteons and does not undergo remodeling, bone formation and resorption occur primarily at the bone surface. Therefore, in this study, the effect of osteoporotic change appeared as a slight reduction in cross-sectional area and not in volumetric BMD. Invariance of BMD in the long bone cortex due to osteoporosis has also been reported in an OVX model [18]. With further aging of Cckbr-deficient mice (e.g., at 52 weeks of age), volumetric BMD should decrease as severe pore formation inside cortical bone occurs [16].

Cholecystokinin (CCK) is a gut–brain peptide that exerts various physiological effects in the gastrointestinal tract and nervous system through cell-surface CCK receptors [23, 24]. CCK receptors have been divided into two subtypes: the CCK-A and CCK-B receptors (CCKBR), both belonging to the class of G protein-coupled receptors characterized by seven transmembrane domains [24].

One role of CCKBR [24–26] includes the stimulation of gastric acid secretion via parietal cells by binding the endogenous peptide hormone gastrin [27, 28]. This has been experimentally confirmed in Cckbr-deficient mice, which mimic gastric hypochlorhydria [16]. Cckbr-deficient mice display gastric hypochlorhydria and calcium malabsorption. Further, calcium deficiency leads to secondary hyperparathyroidism and excessive bone resorption, resulting in an osteoporotic bone phenotype [16]. However, femoral BMD did not differ between Cckbr-deficient and wild-type mice in this study. In contrast, the apatite orientation significantly deteriorated in Cckbr-deficient mice. A previous study reported impaired apatite orientation under hyperparathyroidism in rats with chronic kidney injury [29], and it is possible that hyperparathyroidism itself may have influenced the impaired orientation. However, since uremia also occurred in this model, it should not be concluded that the

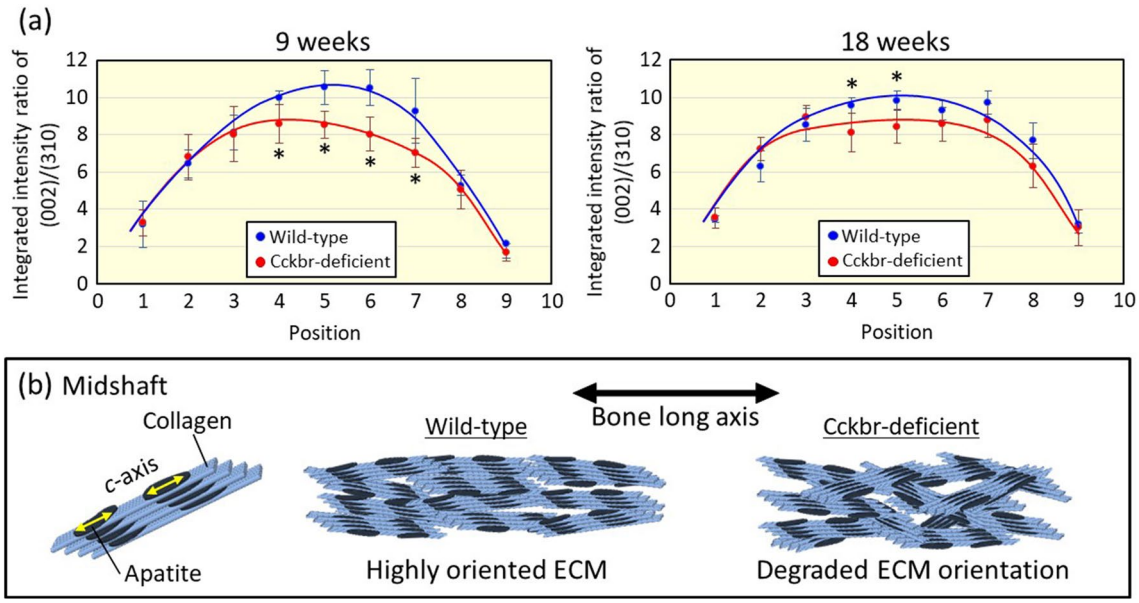

Fig. 6 Comparison of apatite orientation (bone quality parameter). **a** Variation in the preferential orientation of apatite *c*-axis along bone long axis quantitatively analyzed by the intensity ratio of (002) and (310) diffraction peaks and **b** schematic representation of ECM micro-organization for Cckbr-deficient and wild-type mouse femur. $*P < 0.05$

decreased orientation was caused by hyperparathyroidism. Therefore, factors other than hyperparathyroidism that may have contributed to the impaired apatite orientation need to be discussed.

Being mechanosensors, osteocytes are affected by Ca^{2+} signals [30]. Considering that osteocyte morphology and alignment are necessary for the formation of ECM orientation [31], hypocalcemia induced by hypochlorhydria impairs the formation of a preferential ECM orientation. In contrast, a negative correlation has been reported between bone matrix anisotropy and regional periosteal mineral apposition rates [32]. Reports indicated the difference in recovery between BMD and preferential apatite *c*-axis [11], suggesting a discrepancy between the ECM orientation and BMD in this study.

Although BMD measurement did not detect the osteoporotic change due to hypochlorhydria, the assessment of bone quality using ECM orientation did. PPI, which induces hypochlorhydria, is clinically used for gastroesophageal reflux disease, Barrett's esophagus, and non-steroidal anti-inflammatory drug-related bleeding prophylaxis [19]. Therefore, the investigation of PPI-induced osteoporosis is crucial.

In contrast, CCKBR induces pain sensitivity [33, 34]. CCKBR antagonists restored the effectiveness of morphine [35] and attenuated the symptoms of mechanical allodynia in a neuropathic pain model [36]. The upregulation of the opioid system [37] and elevated thresholds of nociceptive stimuli [38] have been observed in Cckbr-deficient mice. Moreover, the deletion of Cckbr reduces mechanical sensitivity [39]. Under unloading conditions, the degree of ECM orientation along the loaded direction significantly degraded [21]. Therefore, mechanical sensitivity may affect the formation of preferential ECM orientations. We considered that the reduction of a specific loading direction of the limbs due to the loss of mechanical sensitivity induced the deterioration of ECM orientation. In Cckbr-deficient mice, hypochlorhydria and deteriorated apatite orientation, which is possibly induced by mechanical hyposensitivity, occur simultaneously, and further investigation is needed to elucidate their direct relationship. Clinically, mechanical sensitivity disorders and specific neuropathies, are induced by diabetes mellitus [40] and spinal disorders [41]. Thus, it is important to examine the effect of mechanical sensitivity on the formation of ECM orientation.

In this study, the deteriorated apatite orientation in Cckbr-deficient mouse femurs partially recovered between 9 and 18 weeks of age. In contrast, the cross-sectional bone area was significantly decreased in 18-week-old but not 9-week-old Cckbr-deficient mice. This decrease in the cross-sectional bone area may compensate for the deterioration of apatite orientation in Cckbr-deficient mice.

Bone changes due to Cckbr-deficiency-induced hypochlorhydria scarcely appeared in bone density throughout the experimental period, appeared in the cross-sectional area (bone mass) at 18 weeks of age, and were detected in the apatite orientation around the mid-shaft as early as 9 weeks of age. This finding provides insight into the early detection of unfavorable bone changes under PPI treatment, which is widely used to induce hypochlorhydria. However, it is necessary to clarify the differences between congenital genetic defects and acquired drug treatments. The method used in this study to analyze the apatite orientation is invasive because bone extraction was required. Recently, a non-invasive method using ultrasound imaging was developed [42], which may be useful for the clinical diagnosis of hypochlorhydria.

In conclusion of this study, we analyzed cross-sectional bone area, BMD, and apatite orientation (a bone quality parameter) in the femoral cortex of Cckbr-deficient and wild-type mice. Deterioration of the apatite preferential orientation in the femur mid-shaft of Cckbr-deficient mice was demonstrated for the first time, despite unchanged BMD. Our results suggest that hypochlorhydria and impaired mechanical sensitivity of Cckbr-deficient mice are at least partially attributable to the degradation of apatite orientation. Moreover, apatite orientation is beneficial in detecting hypochlorhydria induced by PPI treatment, whereas BMD is insensitive.

Acknowledgements This work was supported by CREST-Nanomechanics: Elucidation of macroscale mechanical properties based on understanding nanoscale dynamics for innovative mechanical materials (Grant Number: JPMJCR2194) from the Japan Science and Technology Agency (JST), and a Grant-in-Aid for Scientific Research (JP23H00235) from the Japan Society for the Promotion of Science (JSPS).

Author contributions YM and TN conceptualized and supervised the study and reviewed and edited the manuscript. RO, TO, YY, TY, and AO collected the data. YM and TI wrote the manuscript. All the authors have read and approved the final version of the manuscript.

Declarations

Conflict of interest None.

Ethical approval This study was approved by the Animal Care and Use Committee of Hamamatsu University School of Medicine (approval number: 2019002).

References

1. Chakkalakal DA, Strates BS, Mashoof AA, Garvin KL, Novak JR, Fritz ED, Mollner TJ, McGuire MH (1999) Repair of segmental bone defects in the rat: an experimental model of human fracture healing. Bone 25:321–332
2. Watanabe Y, Takai S, Arai Y, Yoshino N, Hirasawa Y (2002) Prediction of mechanical properties of healing fractures using acoustic emission. J Orthop Res 19:548–553

3. Riggs BL, Melton LJ (2002) Bone turnover matters: the raloxifene treatment paradox of dramatic decreases in vertebral fractures without commensurate increases in bone density, Journal of bone and mineral research. Bone Miner Res 17:11–14
4. Yamamoto M, Yamaguchi T, Yamauchi M, Kaji H, Sugimoto T (2009) Diabetic patients have an increased risk of vertebral fractures independent of BMD or diabetic complications. J Bone Miner Res 24:702–709
5. Ishimoto T, Sato B, Lee JW, Nakano T (2017) Co-deteriorations of anisotropic extracellular matrix arrangement and intrinsic mechanical property in c-src deficient osteopetrotic mouse femur. Bone 103:216–223
6. Gregson CL, Hardcastle SA, Cooper C, Tobias JH (2013) Friend or foe: high bone mineral density on routine bone density scanning, a review of causes and management. Rheumatology 52:968–985
7. Ozasa R, Matsugaki A, Ishimoto T, Kamura S, Yoshida H, Magi M, Matsumoto Y, Sakuraba K, Fujimura K, Miyahara H, Nakano T (2022) Bone fragility via degradation of bone quality featured by collagen/apatite micro-arrangement in human rheumatic arthritis. Bone 155:116261
8. Sekita A, Matsugaki A, Ishimoto T, Nakano T (2017) Synchronous disruption of anisotropic arrangement of the osteocyte network and collagen/apatite in melanoma bone metastasis. J Struct Biol 197:260–270
9. Tuukkanen J, Koivukangas A, Jamsa T, Sundquist K, Mackay CA, Marks SC Jr (2000) Mineral density and bone strength are dissociated in long bones of rat osteopetrotic mutations, Journal of bone and mineral research. Bone Miner Res 15:1905–1911
10. Nakano T, Kaibara K, Tabata Y, Nagata N, Enomoto S, Marukawa E, Umakoshi Y (2002) Unique alignment and texture of biological apatite crystallites in typical calcified tissues analyzed by microbeam X-ray diffractometer system. Bone 31:479–487
11. Ishimoto T, Nakano T, Umakoshi Y, Yamamoto M, Tabata Y (2013) Degree of biological apatite c-axis orientation rather than bone mineral density controls mechanical function in bone regenerated using recombinant bone morphogenetic protein-2. J Bone Miner Res 28:1170–1179
12. Landis WJ (1995) The strength of a calcified tissue depends in part on the molecular structure and organization of its constituent mineral crystals in their organic matrix. Bone 16:533–544
13. Moriishi T, Ozasa R, Ishimoto T, Nakano T, Hasegawa T, Miyazaki T, Liu W, Fukuyama R, Wang Y, Komori H, Qin X, Amizuka N, Komori T (2020) Osteocalcin is necessary for the alignment of apatite crystallites, but not glucose metabolism, testosterone synthesis, or muscle mass. PLoS Genet 16:e1008586
14. Shinno Y, Ishimoto T, Saito M, Uemura R, Arino M, Marumo K, Nakano T, Hayashi M (2016) Comprehensive analyses of how tubule occlusion and advanced glycation end-products diminish strength of aged dentin. Sci Rep 6:19849
15. de Vries F, Cooper AL, Cockle SM, van Staa TP, Cooper C (2009) Fracture risk in patients receiving acid-suppressant medication alone and in combination with bisphosphonates. Osteoporos Int 20:1989–1998
16. Schinke T, Schilling AF, Baranowsky A, Seitz S, Marshall RP et al (2009) Impaired gastric acidification negatively affects calcium homeostasis and bone mass. Nat Med 15:674–681
17. Ozasa R, Ishimoto T, Miyabe S, Hashimoto J, Hirao M, Yoshikawa H, Nakano T (2019) Osteoporosis changes collagen/apatite orientation and Young's modulus in vertebral cortical bone of rat. Calcif Tissue Int 104:449–460
18. Ozasa R, Saito M, Ishimoto T, Matsugaki A, Matsumoto Y, Nakano T (2022) Combination treatment with ibandronate and eldecalcitol prevents osteoporotic bone loss and deterioration of bone quality characterized by nano-arrangement of the collagen/apatite in an ovariectomized aged rat model. Bone 157:116309
19. Freedberg DE, Kim LS, Yang YX (2017) The risks and benefits of long-term use of proton pump inhibitors: Expert review and best practice advice from the American Gastroenterological Association. Gastroenterology 152:706–715
20. Nagata A, Ito M, Iwata N, Kuno J, Takano H, Minowa O, Chihara K, Matsui T, Noda T (1996) G protein-coupled cholecystokinin-B/gastrin receptors are responsible for physiological cell growth of the stomach mucosa in vivo. Proc Natl Acad Sci USA 93:11825–11830
21. Wang J, Ishimoto T, Nakano T (2017) Unloading-induced degradation of the anisotropic arrangement of collagen/apatite in rat femurs. Calcif Tissue Inter 100:87–94
22. Beck TJ, Looker AC, Ruff CB, Sievanen H, Wahner HW (2000) Structural trends in the aging femoral neck and proximal shaft: analysis of the Third National Health and Nutrition Examination Survey dual-energy X-ray absorptiometry data. J Bone Miner Res 15:2297–2304
23. Crawley JN, Corwin RL (1994) Biological actions of cholecystokinin. Peptides 15:731–755
24. Noble F, Roques PB (1999) CCK-B receptor: chemistry, molecular biology, biochemistry and pharmacology. Prog Neurobiol 58:349–379
25. Hughes J, Boden P, Costall B, Domeney A, Kelly E, Horwell DC, Hunter JC, Pinnock RD, Woodruff GN (1990) Development of a class of selective cholecystokinin type B receptor antagonists having potent anxiolytic activity. Proc Natl Acad Sci USA 87:6728–6732
26. Katsuura T (1986) Influences of age and sex on cardiac output during submaximal exercise. Ann Physiol Anthropol 5:39–57
27. Dockray G, Dimaline R, Gastrin AV (2005) Old hormone, new functions. Eur J Physiol 449:344–355
28. Li S, Xue C, Yuan Y, Zhang R, Wang Y, Yu B, Liu J, Ding F, Yang Y, Gu X (2015) The transcriptional landscape of dorsal root ganglia after sciatic nerve transection. Sci Rep 5:e16888
29. Iwasaki Y, Kazama JJ, Yamato H, Matsugaki A, Nakano T, Fukagawa M (2015) Altered material properties are responsible for bone fragility in rats with chronic kidney injury. Bone 81:247–254
30. Hu M, Tian GW, Gibbons DE, Jiao J, Qin YX (2015) Dynamic fluid flow induced mechanobiological modulation of in situ osteocyte calcium oscillations. Arch Biochem Biophys 579:55–61
31. Ishimoto T, Kawahara K, Matsugaki A, Kamioka H, Nakano T (2021) Quantitative evaluation of osteocyte morphology and bone anisotropic extracellular matrix in rat femur. Calcif Tissue Int 109:434–444
32. Kashii M, Hashimoto J, Nakano T, Umakoshi Y, Yoshikawa H (2008) Alendronate treatment promotes bone formation with a less anisotropic microstructure during intramembranous ossification in rats. J Bone Miner Metab 26:24–33
33. Cahill CM, Dray A, Coderre TJ (2003) Intrathecal nerve growth factor restores opioid effectiveness in an animal model of neuropathic pain. Neuropharmacology 45:543–552
34. Cesselin F (1995) Opioid and anti-opioid peptides. Fundam Clin Pharmacol 9:409–433
35. Nichols ML, Bian D, Ossipov MH, Malan TP, Porreca F Jr (1996) Antiallodynic effects of a CCKB antagonist in rats with nerve ligation injury: role of endogenous enkephalins. Neurosci Lett 215:161–164
36. Kovelowski CJ, Ossipov MH, Sun H, Lai J, Malan TP, Porreca F (2000) Supraspinal cholecystokinin may drive tonic descending facilitation mechanisms to maintain neuropathic pain in the rat. Pain 87:265–273
37. Pommier B, Beslot F, Simon A, Pophillat M, Matsui T, Dauge V, Roques BP, Noble F (2002) Deletion of CCK2 receptor in mice results in an upregulation of the endogenous opioid system. J Neurosci 22:2005–2011

38. Veraksits A, Runkorg K, Kurrikoff K, Raud S, Abramov U, Matsui T, Bourin M, Koks S, Vasar E (2003) Altered pain sensitivity and morphine-induced anti-nociception in mice lacking CCK2 receptors. Psychopharmacology 166:168–175
39. Kurrikoff K, Koks S, Matsui T, Bourin M, Arend A, Aunapuu M, Vasar E (2004) Deletion of the CCK2 receptor gene reduces mechanical sensitivity and abolishes the development of hyperalgesia in mononeuropathic mice. Eur J Neurosci 20:1577–1586
40. Vinik AI, Nevoret ML, Casellini C, Parson H (2013) Diabetic neuropathy. Endocrin Metab Clin h Am 42:747–787
41. Yamada T, Yoshii T, Yamamoto N, Hirai T, Inose H, Kato T, Kawabata S, Okawa A (2018) Clinical outcomes of cervical spinal surgery for cervical myelopathic patients with coexisting lumbar spinal canal stenosis (Tandem Spinal Stenosis): a retrospective analysis of 297 cases. Spine 43:E234–E241
42. Ishimoto T, Suetoshi R, Cretin D, Hagihara K, Hashimoto J, Kobayashi A, Nakano T (2019) Quantitative ultrasound (QUS) axial transmission method reflects anisotropy in micro-arrangement of apatite crystallites in human long bones: a study with 3-MHz-frequency ultrasound. Bone 127:82–90